High risk landscapes of Japanese encephalitis virus outbreaks in India converge on wetlands, rainfed agriculture, wild Ardeidae, and domestic pigs

Michael G. Walsh[1,2,3,4], Amrita Pattanaik[5], Navya Vyas[3,4], Deepak Saxena[6], Cameron Webb[2,7], Shailendra Sawleshwarkar[2,3,4,8], Chiranjay Mukhopadhyay[9,10]

[1]The University of Sydney, Faculty of Medicine and Health, School of Public Health, Camperdown, New South Wales, Australia, [2]The University of Sydney, Faculty of Medicine and Health, Sydney Institute for Infectious Diseases, Westmead, New South Wales, Australia, [3]One Health Centre, The Prasanna School of Public Health, Manipal Academy of Higher Education, Manipal, Karnataka, India, [4]The Prasanna School of Public Health, Manipal Academy of Higher Education, Manipal, Karnataka, India, [5]Manipal Institute of Virology, Manipal Academy of Higher Education, Manipal, Karnataka, India, [6]Department of Epidemiology, Indian Institute of Public Health Gandhinagar, Gandhinagar, Gujarat, India, [7]Department of Medical Entomology, NSW Health Pathology, Westmead Hospital, Westmead, New South Wales, Australia [8]The University of Sydney, Faculty of Medicine and Health, Westmead Clinical School, Westmead, New South Wales, Australia, [9]Department of Microbiology, Kasturba Medical College, Manipal Academy of Higher Education, Manipal, Karnataka, India, [10]Centre for Emerging and Tropical Diseases, Kasturba Medical College, Manipal Academy of Higher Education, Manipal, Karnataka, India

*Address correspondence to:
Michael Walsh, PhD, MPH
Senior Lecturer, Infectious Diseases Epidemiology
Marie Bashir Institute for Infectious Diseases and Biosecurity
Sydney School of Public Health
The University of Sydney
176 Hawksbury Road
Westmead NSW 2145 Australia
thegowda@gmail.com
michael.walsh1@sydney.edu.au

Abstract

Japanese encephalitis constitutes a significant burden of disease across Asia, particularly in India, with high mortality in children. This zoonotic mosquito-borne disease is caused by the *Flavivirus*, Japanese encephalitis virus (JEV), and circulates in wild ardeid bird and domestic pig reservoirs both of which generate sufficiently high viremias to infect vector mosquitoes, which can then subsequently infect humans. The landscapes of these hosts, particularly in the context of anthropogenic ecotones and resulting wildlife-livestock interfaces, are poorly understood and thus significant knowledge gaps in the epidemiology and infection ecology of JEV persist, which impede optimal control and prevention of outbreaks. The current study investigated the landscape epidemiology of JEV outbreaks in India over the period 2010 to 2020 based on national human disease surveillance data. Outbreaks were modelled as an inhomogeneous Poisson point process. Outbreak risk was strongly associated with the habitat suitability of ardeid birds and pig density, and shared landscapes between fragmented rainfed agriculture and both river and freshwater marsh wetlands. Moreover, risk scaled with Ardeidae habitat suitability, but was consistent across scale with respect to pig density and rainfed agriculture-wetland mosaics. The results from this work provide a more complete understanding of the landscape epidemiology and infection ecology of JEV in India and suggest important priorities for control and prevention across fragmented terrain comprised of wildlife-livestock interface that favours spillover to humans.

Introduction

Japanese encephalitis virus (JEV) is one of the most substantial causes of childhood encephalitis in Asia(1). While most infections are asymptomatic or mild (approximately 1 in 250 infections present with severe clinical disease), mortality is high among those presenting with encephalitis(1). In India, a country with a high burden of disease caused by JEV, 13.7% of 63,854 acute encephalitis cases from 2010 to 2017 were due to JEV and over 17% of these cases died(2). Although the annual occurrence of Japanese encephalitis (JE) is high, there is considerable heterogeneity in its occurrence across the country with the northeast being a perennial hotspot for outbreaks, although additional far-removed areas of intractable endemicity also persist(2). Japanese encephalitis virus is a mosquito-borne zoonotic *Flavivirus* with enzootic and endemic transmission in animal and human hosts, respectively, although such baseline transmission is regularly punctuated with more substantial outbreaks(3,4). Outbreaks in India are generally seasonal following monsoon flooding, but transmission can and does happen at any time of the year with rural populations typically at highest risk although some urban locations also experience outbreaks(2).

The infection ecology of JEV is complex and incompletely understood in many landscapes. As a result, viral transmission is often poorly controlled. *Culex tritaeniorhynchus* is the most important vector for JEV across Asia(4,5) and has a wide distribution in India(5,6). In addition to this highly efficient vector, there are at least four other important vectors (*Cx. vishnui*, *Cx. gelidus*, *Cx. fuscocephala*, and *Cx. pseudovishnui*) that also exhibit wide distribution across South and Northeast India(6,7). Given the wide range of suitable habitats for these mosquitoes, exposure to JEV vectors is extensive throughout the country. Wading bird species in the Ardeidae family are the primary reservoirs and maintenance hosts for JEV(8–11), while domestic pigs are key amplifying hosts that frequently accelerate spillover to humans(12–17). This general distinction between host groups notwithstanding, high viremias have been shown in several Ardeidae species, so these maintenance hosts may also simultaneously act as

amplifying hosts depending on the nature of their interface with humans or pigs(4). Moreover, some heron species can readily adapt to some agricultural practices (e.g. rice paddies), increasing contact between people and domestic animals in these settings(18). Interestingly, specific maintenance host-mosquito vector-amplifying host interactions have been identified showing *Cx. tritaeniorhynchus* zoophilic feeding preferences for herons and domestic pigs, which may further highlight the importance of interface and the potential for an efficient bridge to human spillover in landscapes that favour these interactions(4).

The biotic factors described above define the vectors and hosts in which JEV circulates and the nature of interspecies interaction that may drive viral transmission dynamics in hosts, but there are equally important abiotic factors that can influence JEV transmission such as wetlands and rainfed agriculture. Heterogenous wetlands not only provide a spectrum of favourable habitat for vectors, they also demarcate critical habitat for key ardeid reservoirs(19). Rainfed agricultural mosaics tend to comprise agricultural systems that 1) are engaged by poorer, subsistence communities, and 2) exhibit far less control of water distribution in the landscape(20). Both wetland habitat and rainfed mosaics can influence mosquito habitats by way of their distribution of water in the landscape, and, since both landscapes can be sensitive to the modulating effects of climate, these could represent important vector foci(21). Moreover, rainfed crop mosaics that lie within or adjacent to wetland habitat may present ecotones of particular risk since these often also present landscapes occupied by key animal hosts and may therefore exhibit multiplicities of JEV transmission (Figure 1). In India, while some states have been recognised as hotspots of annual JEV outbreaks, the landscape epidemiology of JEV has not been thoroughly described in these and other areas of occurrence. The heterogeneity of risk is particularly noteworthy since viable mosquito vectors can be found in most parts of the country. As such, the delineation of JEV outbreak risk across India requires a broader consideration of diverse landscapes, which represent mosaics of wetland habitat, rainfed agriculture, and animal hosts (Figure 1).

Finally, a complete understanding of the epidemiology and infection ecology of JEV requires an understanding of the differential scaling of biotic and abiotic drivers of JEV activity across landscapes. There is some evidence to suggest that biotic interactions between organisms, and abiotic interactions between organisms and their environment (or environmental filtering), may scale differently with respect to some ecological relationships, particularly with respect to pathogen transmission (22). Under this framework, biotic interactions may dominate at more local scale, whereas abiotic interactions can exhibit greater influence at broader scale. However, there is considerable variation with respect to such phenomena, wherein some relationships may show consistency across scale or may show the reverse between biotic and abiotic feature dominance at scale(23). The scaling of risk is an added dimension of JEV epidemiology that has gone unexplored and represents a further critical knowledge gap. Because the scaling of associations may have consequences for epidemiological and ecological inference, or the scale of interventions that may be deployed as a result, it is necessary to examine how associations between biotic and abiotic features may scale differently.

The current study sought to identify the key landscape features of JEV outbreaks in India. In particular, this investigation examined the associations between JEV occurrence in humans and the distribution of maintenance and amplifying animal hosts, wetland hydrogeography and flow dynamics, rainfed agriculture, and climate. These associations were further interrogated at both local and broad scale to determine whether JEV risk scales differently for biotic and abiotic landscape features. While considerable heterogeneity in risk was anticipated, it was hypothesised that river wetlands and rainfed agriculture with high pig density and high Ardeidae suitability would drive the landscape epidemiology of JEV.

Methods

Data sources

The National Centre for Disease Control's Integrated Disease Surveillance Programme (IDSP) maintains ongoing surveillance of JEV infections under the administration of India's Ministry of Health and Family Welfare(24). There were 294 laboratory-confirmed and location-unique outbreaks of JEV reported at village level (spatial resolution of 1 arc minute, or approximately 2 km) to the IDSP between 1 January, 2010 and 31 December, 2020. These were included as the primary training data in the current study. As a test of the external validity of these surveillance data, a secondary dataset (n = 27) comprising all available independent, laboratory-confirmed community surveys of human and mosquito infection conducted within the same time period as the IDSP surveillance and with published location data were used to test the performance of models trained with the IDSP surveillance data(25–28).

JE infections often disproportionally affect communities of lower socioeconomic status with limited access to health care, so this study adjusted for potential reporting bias of JEV infections using the distribution of health system performance as a representation of the local capacity to detect cases (see modelling description below). The infant mortality ratio (IMR) was chosen as a proxy for health system performance since it has been validated as representative of health infrastructure and health system performance and used to assess health service delivery and performance in diverse settings(29,30). Moreover, the IMR is correlated with the Inequality-Adjusted Human Development Index (IHDI) and the Human Development Index (HDI) and is therefore an important representation of the economic, social, and environmental structural determinants of population health(29,31). The raster of the IMR was obtained from the Socioeconomic Data and Applications Center (SEDAC) repository(32). Human population density was derived from the Global Rural-Urban Mapping Project estimates for the 2010 population(33) to represent the baseline population at the beginning of the period under study. The raster data product was obtained from the SEDAC repository.

The Global Biodiversity Information Facility (GBIF) was used to acquire all observations of Ardeidae species (241,784 individual observations of 15 species) between 1 January 2010 and 31 December 2020 across India so each species' distribution could be modelled(34). Pig density data were obtained from the Gridded Livestock of the World(35) (GLW). While pigs been have been demonstrated as key amplifying hosts for JEV, some evidence suggests that poultry may also act as bridging hosts to human spillover in some settings(11,36,37), so we additionally included poultry density in these analyses obtained from the same GLW source. For some regions of the world these data demonstrate non-negligible spatial heterogeneity in error. However in India, the estimates were adjusted by animal censuses at the 2nd and 3rd stage administration levels, corresponding to the district and taluk, respectively, which represented a high level of data verification at a sub-state scale(35).

Due to potential differential accessibility, the background points used to model Ardeidae species distributions were weighted by the human footprint (HFP) (see modelling description below) to correct for potential spatial reporting bias in the observations of these birds. Human footprint raster data were acquired from the SEDAC registry(38) and quantified according to a 2-stage classification system(39). First, a metric for human influence was constructed based on the following eight categories: (1) population density, (2) road proximity, (3) rail line proximity, (4) navigable river poximity, (5) coastline proximity, (6) artificial light at night, (7) rural versus urban location, and (8) land cover. These categories were scored and summed to generate the human influence index (HII), which ranges from 0 (absence of human impact) to 64 (maximum human impact). The ratio of the range of minimum and maximum HII in the local terrestrial biome to the range of minimum and maximum HII across all biomes, expressed as a percentage, is then calculated to produce the HFP metric(39).

The structure of water movement through the landscape was quantified using hydrological flow accumulation obtained from the Hydrological Data and Maps based on SHuttle Elevation Derivatives at multiple Scales (HydroSHEDS) information system (https://hydrosheds.cr.usgs.gov/), which is derived

192 from elevation data of the Shuttle Radar Topography Mission(40). Hydrological flow accumulation
193 measures the quantity of upland area draining into each 500 × 500 m area.
194 Wetlands were classified using the surface water data from the Global Lakes and Wetlands
195 Database(41). Wetland types represented in the current study comprised: coastal wetland, river,
196 controlled water reservoir, lake, freshwater marsh, swamp, or intermittent wetland(42). To quantify
197 proximity to each wetland type, the proximity function in the QGIS geographic information system was
198 used to create distance rasters for each wetland class(43). The pixel values of these rasters represent
199 the distance in kilometres between each wetland type and all other pixels within the geographic extent
200 under study. The distance rasters were then used to investigate the relationships between distinct
201 wetland environments and JEV outbreaks.
202 Agriculture data were obtained from the Global Food Security Support Analysis Data (GFSAD)
203 project to describe the geographic extent of crops that employ rainfed water distribution systems at a
204 resolution of 30 arc seconds(44). Two primary classes of rainfed agricultural systems were represented:
205 dominant rainfed crops and fragmented rainfed crop mosaics. A third class, highly fragmented rainfed
206 crop mosaics, was also available but was highly correlated and exhibited considerable overlap with
207 fragmented mosaics and yielded very similar relationships, so this class was considered redundant and
208 not included in this investigation. As with the wetland classes described above, distance rasters were
209 created for both the dominant rainfed crop and fragmented rainfed crop classes using the proximity
210 function in QGIS.
211 Climate data were obtained from the WorldClim Global Climate database(45). This investigation
212 examined seasonal measures of precipitation due to the distinct seasonal pattern in JEV outbreaks, as
213 particularly marked by monsoon-associated precipitation. Accordingly, rasters for the mean driest
214 quarter precipitation and wettest quarter precipitation, as well as the mean annual temperature, were
215 used in this analysis.

Statistical Analyses

Ardeidae species distribution modelling. An ensemble approach comprising both boosted regression trees (BRT) and random forests (RF) models was used to estimate the landscape suitability of each of the 15 Ardeidae species. Species distribution models (SDMs) based on these machine learning frameworks partition the data space according to algorithms that optimise homogeneity among predictors and a response (e.g. species presence), whereby optimised decision trees are iteratively determined and can capture complex interactions between predictors(46–49). Each SDM under the two distinct modelling frameworks (BRT and RF) was fit using five-fold cross-validation. To prevent artificial spatial clustering of observation data, the data were thinned to include only one observation per pixel in the analysis (S1 Table 1). Mean annual precipitation, mean annual temperature, isothermality, and proximity to surface water comprised the environmental features included in the SDMs. These variables exhibited low correlation with each other (all Pearson's $r < 0.5$) and therefore their inclusion together in the models was justified. Model performance, based on the area under the receiver operating characteristic curve (AUC), and model fit, based on the deviance, were used to evaluate each of the two SDM frameworks (BRT and RF) for each ardeid species. Subsequently, an ensemble landscape suitability was estimated for each species from the two SDM frameworks using their weighted mean, with weights based on AUC(50). Potential spatial sampling bias in the GBIF database was adjusted for by sampling background points proportional to the human footprint as a proxy for landscape accessibility. The landscape suitability for each species was modelled at a spatial resolution of 30 arc seconds (~1 km). Individual species are presented with their number of field observations (and thinned analytical observations) and model metrics in S1 Table 1.

After modelling the distributions of individual Ardeidae species' landscape suitability, a composite of ardeid suitability was calculated based on the mean of all individual species suitability distributions. The degree of niche overlap(51) between each individual species landscape suitability and

240 the composite species suitability was evaluated to determine the extent of heterogeneity between the
241 species-specific environmental niches. More specifically, niche overlap was assessed to determine (1) if
242 heterogeneity was too extensive to justify a composite representation of Ardeidae species landscape
243 suitability, (2) if a small number of ardeid species demonstrating divergent landscape suitability should
244 be considered individually in concert with a composite representation of landscape suitability for the
245 remaining species, or (3) if the species demonstrated sufficient overlap in their environmental niches to
246 justify a composite representation of Ardeidae species landscape suitability alone. The sdm package(50)
247 in the R platform(52) was used for fitting each model and the derivation of the two-model ensembles to
248 each species and the dismo package was used to compare niche overlap(53).
249 *JEV outbreak modelling*. The JEV outbreaks were fitted as a point process using homogeneous
250 and inhomogeneous Poisson models(54). This framework allows for the assessment of spatial
251 dependencies among the outbreaks and, where such dependencies are identified, these can be
252 evaluated with respect to environmental features that may account for the observed dependencies.
253 First, JEV outbreaks were fitted as a homogeneous Poisson process, with conditional intensity,
254 $$\lambda(u,X) = \beta, \qquad (1)$$
255 where u designates the geographic locations of outbreaks, X, and β represents the intensity parameter.
256 Intensity is defined as the number of points in a subregion of a defined geographic extent. The
257 homogeneous Poisson model is the null model representing complete spatial randomness (CSR). Under
258 CSR, the expected intensity is proportional to the area of the subregion under consideration(54), i.e.,
259 there is no spatial dependency.
260 Second, the model with the assumption of CSR was compared to an inhomogeneous Poisson
261 process, which incorporates spatial dependency of the outcome (JEV outbreaks) into the model
262 structure and has conditional intensity,
263 $$\lambda(u,X) = \beta(u). \qquad (2)$$

With this model, the intensity is represented as a function of the location, u, of the JEV outbreaks. The inhomogeneous Poisson model supported substantive spatial dependency in JEV outbreak intensity as this was a markedly better fit than the CSR model and also demonstrated significant divergence from CSR in the K-function (see results below). Given the identified spatial dependence in JEV outbreaks, simple and multiple inhomogeneous Poisson models with environmental features were fitted with conditional intensity,

$$\lambda(u,X) = \rho\,(Z(u)), \qquad (3)$$

where ρ is the parameter representing the association between the point intensity and the feature Z at location u. The models' background points were sampled proportional to IMR, as described above, to control for potential reporting bias in the JEV infection surveillance.

As above for the SDMs, the outbreak occurrences were thinned to prevent over-fitting of the models. The data were thinned so that no more than one event was included within each pixel under the two spatial scales investigated at 1.0 and 10.0 arc minutes, respectively (see below). In addition, the environmental covariates were aggregated for these same two spatial scales, 1.0 and 10.0 arc minutes, respectively. Human population density was included in all models as an offset so that the models appropriately represented epidemiological risk. The crude associations between JEV outbreaks and mean dry quarter precipitation, mean wet quarter precipitation, mean annual temperature, hydrological flow accumulation, proximity to each wetland type, proximity to rainfed agricultural systems, the composite landscape suitability of Ardeidae species, pig density, and poultry density were initially assessed individually with a separate simple inhomogeneous Poisson model (S2 Table 2). Features demonstrating bivariate associations with confidence intervals that did not include 0 were included as covariates in the multiple inhomogeneous Poisson models (S3 Figure 1, S4 Figure 2, S5 Figure 3). The features included as covariates in the multiple inhomogeneous Poisson models demonstrated low correlation (all values of the Pearson's r were <0.5) and so were deemed appropriate to be included

288 together in the models. The associations between JEV outbreaks and landscape features were
289 represented by relative risks, which were computed from the regression coefficients of the
290 inhomogeneous Poisson models. Interaction between fragmented rainfed agriculture and the two
291 dominant wetland types, river and freshwater marsh, were examined separately using a river-rainfed
292 crops model and a freshwater marsh-rainfed crops model with a corresponding interaction term
293 included in each model, respectively. In this way, the interaction between fragmented rainfed
294 agriculture and both river and freshwater marsh wetlands was used to evaluate the impact of their
295 shared landscape mosaics on JEV risk. The Akaike information criterion (AIC) assessed model fit, while
296 the AUC assessed model performance. Importantly, model performance was tested against an
297 independent, laboratory-confirmed dataset derived from the community-based surveys described
298 above. The use of independent data for testing model performance provides a test of the external
299 validity of the results thereby improving model assessment considerably. Model selection was based on
300 a comparison the fit (based on AIC) of the full model to reduced model groups nested on three broad
301 environmental domains (hydrogeography, animal hosts, and climate). These were also compared against
302 a stepwise selection procedure with the full point process model to see if there was any divergence in
303 model selection(55,56). Assessment of K-functions fitted to the JEV outbreaks before and after point
304 process modelling with the specified environmental features was used to determine if these features
305 adequately accounted for the observed spatial dependencies.
306 As described above, the influence of biotic and abiotic features have been shown to scale
307 differently for some pathogen systems(22). To account for such scaling in the current investigation,
308 models were fitted and assessed at local (1.0 arc minutes) and broad (10.0 arc minutes) scales. Likewise,
309 model fit (AIC) and performance (AUC) were also compared across scales. The R statistical software
310 version 3.6.1 was used to perform the analyses(52). Point process models were fitted and K-functions

311 estimated using the spatstat package(55,56). The silhouette images of Ardeidae, pigs, mosquitoes, and
312 rice in Figure 1 were acquired from phylopic.org and used under Creative Commons license.
313
314 Results
315 The landscape suitability of individual Ardeidae species demonstrated a high degree of overlap
316 with the composite landscape suitability (niche overlap > 88% for all species, and > 96% for all but one
317 species; S1 Table 1), so the composite measure of Ardeidae suitability was used in the modelling of JEV
318 outbreaks.
319 At 1.0 arc minute (~ 2 km), the best fitting and performing models of JEV outbreak risk under
320 fragmented rainfed mosaics with freshwater marsh and fragmented rainfed mosaics with river were the
321 reduced models 7 and 8, respectively, which excluded poultry (S6 Table S3; Table 1). These final models
322 were further supported by the stepwise selection procedure implemented with the point process
323 models. Japanese encephalitis virus outbreaks were strongly associated with both Ardeidae suitability
324 (Table 1 Model 1 - RR = 1.14, 95%C.I. 1.07 – 1.21; Model 2 - RR = 1.13, 95%C.I. 1.06 – 1.21) and pig
325 density (Model 1 - RR = 1.41, 95%C.I. 1.33 – 1.51; Model 2 - RR = 1.40, 95%C.I. 1.31 – 1.49), whereby an
326 increasing presence of both in the landscape was associated with increased risk. Proximity to
327 fragmented rainfed agricultural mosaics (Table 1, Model 1 - RR = 0.978 and Model 2 - RR = 0.979) was
328 associated with increased risk of JEV outbreaks (inverse associations indicate increasing distance from
329 this feature was associated with decreasing risk and vice versa), but not proximity to major non-
330 fragmented rainfed agricultural systems (S2 Table 2). Importantly, proximity to both river and
331 freshwater marsh wetlands were also strongly associated with increased risk, and each modified the
332 association between JEV outbreaks and fragmented rainfed crop mosaics, such that proximity to the
333 rainfed mosaics was associated with risk only in locations where the mosaics were shared with, or
334 adjacent to, the two wetland habitats (Table 1). As expected, climate, especially precipitation, was also

strongly associated with JEV outbreaks. Estimates of the distribution of JEV outbreak risk with 95% confidence limits are presented in Figure 3. The spatial dependency apparent in JEV outbreaks as estimated by the homogenous K-function (left panels, Figure 4) was largely accounted for by the final inhomogeneous Poisson models (right panels, Figure 4).

At 10.0 arc minutes JEV outbreaks continued to demonstrate strong associations with pig density, wetlands and fragmented rainfed mosaics, and precipitation, however Ardeidae suitability and temperature did not continue to manifest influence at this broad scale (S7 Table 4).

Discussion

This is the first investigation of JEV outbreaks to consider the impact of shared landscapes with key wildlife and domesticated animal reservoirs for JEV, while simultaneously assessing the convergence of natural wetland habitat with rainfed agriculture. Moreover, these landscape features were evaluated at multiple scales to determine whether their influence manifested differently at local and broad scales. Both wild ardeid and domestic pig hosts were strongly associated with JEV outbreak risk at local scale. However, at broad scale only pigs continued to manifest a broad footprint in the landscape. River and freshwater marsh systems and their shared landscapes with fragmented rainfed agriculture were also strongly associated with outbreak risk at both local and broad scale. These differences in risk between animal hosts and the environment demonstrate the importance of considering the ways in which biotic and abiotic features, respectively, comprise complex risk landscapes for JEV that vary with scale. Moreover, these could have potentially important policy implications for the control and prevention of outbreaks. For example, factors that dominate locally such as the sharing of space between ardeid birds and domestic pigs might be ideally targeted for intervention by local municipalities, whereas factors that dominate at broader scale, such as veterinary surveillance of pigs or the development of a novel pig vaccination program, may be more effectively targeted and resourced by state or national authorities.

The family Ardeidae comprises the wading birds, herons (including egrets) and bitterns. Ardeid birds have been recognised as key maintenance hosts for JEV(8–11). Domestic pigs, conversely, are important amplification hosts due to the high viremia associated with porcine infection(12–17). Pigs are also important since these are livestock animals and typically occupy space in close proximity to humans, although several heron species, such as the cattle egret, *Bubulcus ibis*, are also capable of thriving in anthropogenic landscapes(57). Therefore, as expected, both of these wild and domesticated animal hosts were strongly associated with outbreak risk at local scale in the current study. Interestingly, the influence of Ardeidae suitability appeared to manifest only at local scale, whereas pig density was associated with risk at local and broad scale. The difference in scaling of ardeid and pig hosts may reflect differences in the influence of Ardeidae-pig interfaces at different scales, whereby the influence of domestic pigs on JEV outbreaks may manifest regionally beyond the local impact of their interface with ardeid hosts, whereas the influence of the ardeid hosts may be confined to their local interface with pigs. Importantly, the current study did not observe and assess specific interactions between ardeid birds and pigs across India, which precludes any definitive conclusions about the roles of these hosts in the infection ecology of JEV at different scales of influence. Field investigations of interspecific interactions in local settings will be required to verify the results from the current study and ultimately define how different classes of hosts operate with respect to viral circulation and spillover at scale.

Wetlands can provide important habitat for mosquitoes and therefore increased outbreak risk associated with the provision of a stable source of surface water in these habitats is intuitive. Nevertheless, wetland systems are not homogeneous geomorphologically or ecologically, and neither were they homogeneous with respect to JEV occurrence as clearly demonstrated by the lack of association between outbreak risk and proximity to any surface water type (S2 Table 2). Instead, river and freshwater marsh wetlands dominated JEV outbreak risk, with both also demonstrating interaction with fragmented rainfed agriculture suggesting that shared landscapes of wetland habitat and

fragmented rainfed mosaics may be particularly important to the landscape epidemiology of JEV outbreaks. These associations are intuitive because wetland-rainfed agricultural mosaics may represent landscapes of more seasonally stable precipitation compared to rainfed crops that are far removed from wetland habitat. This was further supported by the strong and independent association with precipitation that was observed at both local and broad scale. Furthermore, fragmented rainfed mosaics within or adjacent to wetlands may also demarcate landscapes with limited control of water dispersal following inundation(20), which is particularly relevant to the annual monsoon flooding and which corresponds to the season of highest JEV incidence. It is also important to note that rainfed agriculture is typically a system employed by resource-limited subsistence farmers, with fragmented agricultural landscapes often corresponding to more economically disadvantaged communities(20), and which also tend to represent a preponderance of the annual JEV incident cases(2). Therefore, not only do these findings provide further insight into the epidemiology of JEV outbreaks, they also identify vulnerable communities that are likely to be at greatest risk and which may yield maximum benefit from targeted resource allocation to prevent future outbreaks.

As expected, increasing precipitation was associated with increased JEV outbreak risk at both local and broad scale. Interestingly, temperature was inversely associated JEV outbreak risk at local scale, but demonstrated no association at broad scale. While JEV outbreaks were widely distributed across India, there was a preponderance of occurrence in the wettest areas of the country, which also tend to coincide with areas of slightly lower mean annual temperature and may reflect this inverse association at local scale. Alternatively, areas of more extreme heat in India may exist within a temperature spectrum that is less favourable to the provision of habitat for reservoirs and vectors, to vector development and longevity, to the extrinsic incubation period in vectors, or the areas of highest temperature regimes may simply be coincident with precipitation and humidity regimes that are less favourable(4). Regardless, these associations are based on climate rather than weather. As such, future

work will need to explore the effects of specific weather events and patterns with the requisite temporal resolution to link fluctuations in precipitation and temperature with individual JEV outbreaks. For example, one study examined a long-term time series of JEV occurrence and found that increases in both rainfall and temperature were associated with increased risk(21). However, this work was limited to one district in one state, so more work will require examination across many more of India's heterogenous landscapes to better understand how weather fluctuation may operate in different landscapes. Nevertheless, the association between JEV and precipitation has shown broad geographical consistency as manifested in China, for example, where cases were mostly concentrated in landscapes with annual precipitation greater than 400 mm irrespective of whether these landscapes were characterised by warm-temperate, semitropical or tropical climate regimes(58).

It is important to acknowledge and discuss some additional limitations attending this work. First, although the national IDSP surveillance system was used to capture all reported outbreaks under investigation, we recognise that reporting bias may still be present. To correct for potential reporting bias, rather than randomly selecting background points for the point process models, background sampling was instead weighted by the distribution of IMR as a robust indicator of health system accessibility and infrastructure. Second, the species distribution models used to construct Ardeidae suitability were based on human observations and so are also subject to reporting bias, insofar as bird accessibility is likely to impact reporting effort. Reporting bias in Ardeidae observations was corrected by weighting the sampling of background points by HFP as an indicator of accessibility. In addition, while this study was able to estimate the landscape suitability of several Ardeidae species, there were some species for which there were too few observations to validly model suitability. As such, we concede that this work is not an exhaustive representation of all possible species niches and therefore some aspects may yet remain undescribed by these findings. Third, the climate measures interrogated in the models presented were based on decadal averages over the period from 1950 to 2000, which assumes

431 homogeneity over this time period as well as over the period of JEV outbreak surveillance under
432 investigation. However, the current study sought to model the influence of climate features in the
433 landscape rather than specific weather events, so these assumptions were deemed appropriate.
434 This study showed that JEV risk in India was strongly associated with the distribution of animal
435 hosts and the shared landscapes between fragmented rainfed agriculture and river and freshwater
436 marsh wetlands. Importantly, animal hosts operated with different degrees of influence at local and
437 broad scale, which may provide unique opportunities to target distinct aspects of JEV landscape
438 epidemiology with differential resource allocation by local and state (or national) municipalities,
439 respectively, to optimise control and prevention of JEV outbreaks. For example, the World Health
440 Organisation has outlined potential forms of landscape manipulation and modification, such as the
441 rotation or synchronisation of crop cycles, alternating crop varieties with variable growing seasons, or
442 mechanical intervention on water movement through the landscape to subvert vector breeding(59).
443 Moreover, the mitigation of vector abundance directly associated with rainfed agriculture may be
444 negated where wetland habitat is present (i.e. in fragmented mosaics) representing a refuge for
445 mosquitoes from control measures and therefore a need for increased attention. Alternatively, there
446 may be opportunities for the repositioning of livestock animal pens at sites more distal to human
447 residences, or locations of agricultural activity, to limit the vector-animal-human interface(59). These
448 kinds of hyperlocal interventions could be ideally suited to administration by local municipalities such as
449 the sub-district taluks (tehsils), particularly since such interventions often require working closely with
450 affected communities. In contrast, broader interventions such as those involving resource-intensive
451 vaccination campaigns of humans (or livestock) may be more effectively orchestrated at the state or
452 national levels. The findings highlight the importance of developing collaborative surveillance
453 infrastructure for vectors, animals, and humans across scale such that an effective surveillance system
454 will require operation and communication within and between taluks, districts, and states. These

455 surveillance systems should also remain adaptive to the influence of land use change, climate change,
456 and urbanisation that may also influence future risks of JEV in India.
457
458
459
460
461
462
463
464
465
466
467
468
469
470
471
472
473
474
475
476
477
478
479
480
481
482

References

1. Organization WH. Japanese encephalitis vaccines: WHO position paper. Wkly Epidemiol Rec. 2015;90:69–87.

2. National vectorborne Disease Control Program, Ministry of Health and Family Welfare G of I. Statewise number of AES/JE cases and deaths from 2010–2017. 2017;

3. Mackenzie JS, Barrett A, Deubel V. The Japanese Encephalitis Serological Group of Flaviviruses: a Brief Introduction to the Group. In: Mackenzie JS, Barrett A, Deubel V, editors. Japanese Encephalitis and West Nile Viruses. Berlin: Springer-Verlag; 2002. p. 1–10.

4. Endy TP, Nisalak A. Japanese Encephalitis Virus: Ecology and Epidemiology. In: Mackenzie JS, Barrett A, Deubel V, editors. Japanese Encephalitis and West Nile Viruses. Berlin: Springer-Verlag; 2002. p. 11–48.

5. Longbottom J, Browne AJ, Pigott DM, Sinka ME, Golding N, Hay SI, et al. Mapping the spatial distribution of the Japanese encephalitis vector, Culex tritaeniorhynchus Giles, 1901 (Diptera: Culicidae) within areas of Japanese encephalitis risk. Parasites and Vectors. 2017;10(1):1–12.

6. Samy AM, Alkishe AA, Thomas SM, Wang L, Zhang W. Mapping the potential distributions of etiological agent, vectors, and reservoirs of Japanese Encephalitis in Asia and Australia. Acta Trop [Internet]. 2018;188(August):108–17. Available from: https://doi.org/10.1016/j.actatropica.2018.08.014

7. Thankachy S, Dash S, Sahu SS. Entomological factors in relation to the occurrence of Japanese encephalitis in Malkangiri district, Odisha State, India. Pathog Glob Health [Internet]. 2019;113(5):246–53. Available from: https://doi.org/10.1080/20477724.2019.1670926

8. Rodrigues FM, Guttikar SN, Pinto BD. Prevalence of antibodies to Japanese encephalitis and West Nile viruses among wild birds in the Krishna-Godavari Delta, Andhra Pradesh, India. Trans R Soc Trop Med Hyg. 1981;75(2):258–62.

9. Jamgaonkar A V., Yergolkar PN, Geevarghese G, Joshi GD, Joshi M V., Mishra AC. Serological evidence for Japanese encephalitis virus and West Nile virus infections in water frequenting and terrestrial wild birds in Kolar District, Karnataka State, India. A retrospective study. Acta Virol. 2003;47(3):185–8.

10. Buescher EL, Scherer WF, Rosenberg MZ, Kutner LJ. Immunologic studies of Japanese encephalitis virus in Japan. IV. Maternal antibody in birds. J Immunol. 1959;83:614–9.

11. Bhattacharya S, Basu P. Japanese Encephalitis Virus (JEV) infection in different vertebrates and its epidemiological significance: a Review. Int J Fauna Biol Stud [Internet]. 2014;1(6):32–7. Available from: https://pdfs.semanticscholar.org/51c4/860d8c66c5fa9d730143e836b8db0b21c1a4.pdf

12. Baruah A, Hazarika R, Barman N, Islam S, Gulati B. Mosquito abundance and pig seropositivity as a correlate of Japanese encephalitis in human population in Assam, India. J Vector Borne Dis. 2018;55(4):291–6.

13. Borah J, Dutta P, Khan SA, Mahanta J. Epidemiological concordance of Japanese encephalitis virus infection among mosquito vectors, amplifying hosts and humans in India. Epidemiol Infect. 2013;141(1):74–80.

14. Kakkar M, Chaturvedi S, Saxena VK, Dhole TN, Kumar A, Rogawski ET, et al. Identifying sources, pathways and risk drivers in ecosystems of Japanese Encephalitis in an epidemic-prone north Indian district. PLoS One. 2017;12(5):1–17.

15. Chen B, Beaty B. Japanese encephalitis vaccine (2-8 strain) and parent (SA 14 strain) viruses in Culex tritaeniorhynchus mosquitoes. Am J Trop Med Hyg. 1982;31:403–7.

16. Komada K, Sasaki N, Inoue Y. Studies of live attenuated Japanese encephalitis vaccine in swine. J Immunol. 1968;100:194–200.

17. Ghimire S, Dhakal S, Ghimire NP, Joshi DD. Pig Sero-Survey and Farm Level Risk Factor Assessment for Japanese Encephalitis in Nepal. Int J Appl Sci Biotechnol. 2014;2(3):311–4.

18. Le Flohic G, Porphyre V, Barbazan P, Gonzalez J-P. Review of Climate, Landscape, and Viral Genetics as Drivers of the Japanese Encephalitis Virus Ecology. Johansson MA, editor. PLoS Negl Trop Dis [Internet]. 2013 Sep 12 [cited 2021 Aug 27];7(9):e2208. Available from: https://dx.plos.org/10.1371/journal.pntd.0002208

19. del Hoyo J, Elliott A, Vicens JS, Christie DA. Handbook of the Birds of the World [Internet]. Elliott A, Vicens JS, del Hoyo J, editors. Vols. 1-17. Barcelona: Lynx Edicions; 2013 [cited 2020 Jun 23]. Available from: https://www.lynxeds.com/product-category/by-categories/encyclopedias/hbw/

20. Devendra C. Rainfed agriculture: its importance and potential in global food security. Utar Agric Sci J. 2016;2(2):4–17.

21. Singh H, Singh N, Mall RK. Japanese Encephalitis and Associated Environmental Risk Factors in Eastern Uttar Pradesh: A time series analysis from 2001 to 2016. Acta Trop [Internet]. 2020;212(May):105701. Available from: https://doi.org/10.1016/j.actatropica.2020.105701

22. Cohen JM, Civitello DJ, Brace AJ, Feichtinger EM, Ortega CN, Richardson JC, et al. Spatial scale modulates the strength of ecological processes driving disease distributions. Proc Natl Acad Sci [Internet]. 2016;113(24):E3359–64. Available from: http://www.pnas.org/lookup/doi/10.1073/pnas.1521657113

23. Becker DJ, Washburne AD, Faust CL, Mordecai EA, Plowright RK. The problem of scale in the prediction and management of pathogen spillover. Philos Trans R Soc B Biol Sci. 2019;374(1782):20190224.

24. National Centre for Disease Control, Directorate General of Health Services, Ministry of Health and Family Welfare. Integrated Disease Surveillance Programme(IDSP) [Internet]. [cited 2020 Sep 3]. Available from: https://idsp.nic.in/

25. Balakrishnan A, Thekkekare R, Sapkal G, Tandale B. Seroprevalence of Japanese encephalitis virus & West Nile virus in Alappuzha district, Kerala. Indian J Med Res [Internet]. 2017 Jul 1 [cited 2021 Jul 21];146(7):70. Available from: http://www.ijmr.org.in/text.asp?2017/146/7/70/219461

26. Dwibedi B, Mohapatra N, Rathore S, Panda M, Pati S, Sabat J, et al. An outbreak of Japanese encephalitis after two decades in Odisha, India. Indian J Med Res [Internet]. 2015 Dec 1 [cited 2021 Jul 21];142(7):30. Available from: http://www.ijmr.org.in/text.asp?2015/142/7/30/176609

27. Ramesh D, Muniaraj M, Samuel Pp, Thenmozhi V, Venkatesh A, Nagaraj J, et al. Seasonal abundance & role of predominant Japanese encephalitis vectors Culex tritaeniorhynchus & Cx. gelidus Theobald in Cuddalore district, Tamil Nadu. Indian J Med Res [Internet]. 2015 Dec 1 [cited

2021 Jul 21];142(7):29. Available from: http://www.ijmr.org.in/text.asp?2015/142/7/23/176607

28. Nyari N, Singh D, Kakkar K, Sharma S, Pandey SN, Dhole TN. Entomological and serological investigation of Japanese encephalitis in endemic area of eastern Uttar Pradesh, India. J Vector Borne Dis. 2015;52(4):321–8.

29. Reidpath DD, Allotey P. Infant mortality rate as an indicator of population health. J Epidemiol Community Health [Internet]. 2003 May 1 [cited 2020 Jul 14];57(5):344–6. Available from: https://pubmed.ncbi.nlm.nih.gov/12700217/

30. Choi J, Ki M, Kwon HJ, Park B, Bae S, Oh C-M, et al. Health Indicators Related to Disease, Death, and Reproduction. J Prev Med Public Heal [Internet]. 2019 Jan 31 [cited 2020 Jul 14];52(1):14–20. Available from: http://jpmph.org/journal/view.php?doi=10.3961/jpmph.18.250

31. Ignacio Ruiz J, Nuhu K, Tyler McDaniel J, Popoff F, Izcovich A, Martin Criniti J. Inequality as a powerful predictor of infant and maternal mortality around the world. PLoS One [Internet]. 2015 Oct 21 [cited 2020 Jul 14];10(10). Available from: https://pubmed.ncbi.nlm.nih.gov/26488170/

32. Center for International Earth Science Information Network - CIESIN - Columbia University. Global Subnational Infant Mortality Rates, Version 2 [Internet]. Palisades; 2019. Available from: https://doi.org/10.7927/H4PN93JJ

33. Center for International Earth Science Information Network - CIESIN - Columbia University, International Food Policy Research Institute - IFPRI, The World Bank and CI de AT-C. Population Density Grid, v1: Global Rural-Urban Mapping Project (GRUMP), v1 | SEDAC [Internet]. Palisades, NY: NASA Socioeconomic Data and Applications Center (SEDAC). [cited 2014 Oct 23]. Available from: http://sedac.ciesin.columbia.edu/data/set/grump-v1-population-density

34. GBIF. GBIF occurrence download - Ardeidae India [Internet]. Global Biodiversity Information Facility. 2021. Available from: https://doi.org/10.15468/dl.s99zmx

35. Robinson TP, Wint GRW, Conchedda G, Van Boeckel TP, Ercoli V, Palamara E, et al. Mapping the global distribution of livestock. PLoS One [Internet]. 2014 Jan [cited 2015 May 26];9(5):e96084. Available from: http://www.pubmedcentral.nih.gov/articlerender.fcgi?artid=4038494&tool=pmcentrez&rendertype=abstract

36. Ogata M, Nagao Y, Jitsunari F, Kitamura N, Okazaki T. Infection of herons and domestic fowls with Japanese encephalitis virus with specific reference to maternal antibody of hen (epidemiological study on Japanese encephalitis 26). Acta Med Okayama. 1970;24:175–84.

37. Bhattacharya S, Chakraborty S, Chakraborty S, Ghosh K, Palit A, Mukherjee K, et al. Density of Culex vishnui and appearance of JE antibody in sentinel chicks and wild birds in relation to Japanese encephalitis cases. Trop Geogr Med [Internet]. 1988 [cited 2021 Aug 13];38(1):46–50. Available from: https://pubmed.ncbi.nlm.nih.gov/3008391/

38. Socioeconomic Data and Applications Center | SEDAC. Methods» Last of the Wild, v2 | SEDAC [Internet]. [cited 2014 Dec 23]. Available from: http://sedac.ciesin.columbia.edu/data/collection/wildareas-v2/methods

39. Sanderson EW, Jaiteh M, Levy MA, Redford KH, Wannebo A V, Woolmer G. The Human Footprint and the Last of the Wild. 2002;52(10).

40. Lehner B, Verdin K, Jarvis A. HydroSHEDS Technical Documentation [Internet]. 2006. Available from: http://hydrosheds.cr.usgs.gov

41. Fund WW. Global Lakes and Wetlands Database [Internet]. Available from: http://www.worldwildlife.org/pages/global-lakes-and-wetlands-database

42. Lehner B, Döll P. Development and validation of a global database of lakes, reservoirs and wetlands. J Hydrol. 2004 Aug;296(1-4):1–22.

43. QGIS Development Team. QGIS Geographic Information System [Internet]. Open Source Geospatial Foundation; 2009. Available from: http://www.qgis.org/

44. Thenkabail P, Teluguntla P, Xiong J, Oliphant A, Massey R. LP DAAC - GFSAD1KCM [Internet]. Global Food Security Support Analysis Data (GFSAD) Crop Mask 2010 Global 1 km V001. 2016 [cited 2021 Jul 21]. Available from: https://lpdaac.usgs.gov/products/gfsad1kcmv001/

45. WorldClim - Global Climate. Data for current conditions (~1950-2000) | WorldClim - Global Climate Data [Internet]. WorldClim - Global Climate Data. [cited 2014 Oct 23]. Available from: http://www.worldclim.org/current

46. Elith J, Leathwick JR, Hastie T. A working guide to boosted regression trees. J Anim Ecol. 2008 Jul;77(4):802–13.

47. Friedman J. Greedy function approximation: a gradient boosting machine. Ann Stat. 2001;29(5):1189–232.

48. Breiman L. Random forests. Mach Learn. 2001;45(1):5–32.

49. James G, Witten D, Hastie T, Tibshirani R. An introduction to Statistical Learning. Vol. 7, Current medicinal chemistry. 2000. 303-321 p.

50. Naimi B, Araújo MB. sdm: a reproducible and extensible R platform for species distribution modelling. Ecography (Cop) [Internet]. 2016 Apr 1 [cited 2021 Feb 12];39(4):368–75. Available from: http://doi.wiley.com/10.1111/ecog.01881

51. Warren DL, Glor RE, Turelli M. Environmental niche equivalency versus conservatism: quantitative approaches to niche evolution. Evolution [Internet]. 2008 Nov [cited 2018 Jun 7];62(11):2868–83. Available from: http://doi.wiley.com/10.1111/j.1558-5646.2008.00482.x

52. R Core Team. R: A language and environment for statistical computing [Internet]. Vienna: R Foundation for Statistical Computing; 2016. Report No.: 3.1.3. Available from: https://www.r-project.org/

53. Hijmans RJ, Phillips S, Leathwick JR, Elith J. Package “dismo.” The Comprehensive R Archive Network. 2014. p. 1–65.

54. Baddeley A, Turner R. Practical Maximum Pseudolikelihood for Spatial Point Patterns (with Discussion). Aust <html_ent glyph=“@amp;” ascii=“&”/> New Zeal J Stat [Internet]. 2000 Sep [cited 2014 Oct 23];42(3):283–322. Available from: http://doi.wiley.com/10.1111/1467-842X.00128

55. Baddeley A, Turner R. spatstat: An R Package for Analyzing Spatial Point Patterns. J Stat Softw 12(6) [Internet]. 2005 [cited 2014 Oct 23]; Available from: http://www.jstatsoft.org/v12/i06/

56. Baddeley A, Rubak E, Turner R. Spatial Point Patterns: Methodology and Applications with R [Internet]. Vol. 11. CRC Press; 2015 [cited 2016 Feb 5]. 810 p. Available from: https://books.google.com/books?id=rGbmCgAAQBAJ&pgis=1

57. BirdLifeInternational. Bubulcus ibis [Internet]. The IUCN Red List of Threatened Species 2015: e.T22697109A60156122. 2015. Available from: https://www.iucnredlist.org/species/22697109/60156122

58. HUANG XX, YAN L, GAO XY, REN YH, FU SH, CAO YX, et al. The Relationship between Japanese Encephalitis and Environmental Factors in China Explored Using National Surveillance Data. Vol. 31, Biomedical and Environmental Sciences. Elsevier Ltd; 2018. p. 227–32.

59. World Health Organization. Agricultural Development and Vector-Borne Diseases [Internet]. Training and Information Materials and Vector Biology and Control. 1996. Available from: https://www.who.int/water_sanitation_health/resources/agridevbegin.pdf

671 Table 1. Adjusted relative risks and 95% confidence intervals for the associations between Japanese
672 encephalitis virus (JEV) outbreaks and each landscape feature as derived from the best fitting
673 inhomogeneous Poisson models. Each landscape feature is adjusted for all others in each of the two
674 models. Models are at a scale of 1.0 arc minutes (~2 km).

Landscape feature	**Relative risk**	**95% confidence interval**	**p-value**
Model 1 – Freshwater marsh-rainfed mosaics interaction			
Ardeidae landscape suitability (deciles)	1.14	1.07 – 1.21	0.00005
Pig density (deciles)	1.41	1.33 – 1.51	<0.00001
Distance to river (2 km)	0.74	0.56 – 0.99	0.02
Distance to freshwater marsh (2 km)	0.71	0.63 – 0.82	<0.00001
Distance to fragmented rainfed agriculture	0.978	0.969 – 0.987	<0.00001
Freshwater marsh:fragmented rainfed agriculture	1.008	1.003 – 1.014	0.0007
Mean precipitation during the wettest quarter (10 cm)	1.008	1.006 – 1.009	<0.00001
Mean precipitation during the driest quarter (10 cm)	1.14	1.08 – 1.19	<0.00001
Mean annual temperature (Celsius)	0.90	0.85 – 0.96	0.002
Model 2 – River-rainfed mosaics interaction			
Ardeidae landscape suitability (deciles)	1.13	1.06 – 1.21	0.00005
Pig density (deciles)	1.40	1.31 – 1.49	<0.00001
Distance to river (2 km)	0.63	0.46 – 0.85	0.001
Distance to freshwater marsh (2 km)	0.78	0.70 – 0.88	<0.00001
Distance to fragmented rainfed agriculture	0.979	0.971 – 0.987	<0.00001
River:fragmented rainfed agriculture	1.012	1.006 – 1.017	0.00003
Mean precipitation during the wettest quarter (10 cm)	1.007	1.006 – 1.009	<0.00001
Mean precipitation during the driest quarter (10 cm)	1.14	1.09 – 1.19	<0.00001
Mean annual temperature (Celsius)	0.91	0.86 – 0.97	0.0009

675
676
677
678
679
680
681
682
683
684
685
686

687 Figure legends

688 Figure 1. Theoretical representation of landscapes with wetland (A) and rainfed crop (B) mosaics and
689 their potential animal host occupants. Multiple transmission cycles of Japanese encephalitis virus (JEV)
690 may be realised in such landscapes such as transmission among Ardeidae maintenance hosts (C1),
691 shared transmission between ardeid birds and domestic pigs at the wildlife-livestock interface (C2), and
692 concentrated transmission among porcine amplification hosts (C3).

693 Figure 2. The spatial (left) and temporal (right) distributions of Japanese encephalitis virus (JEV)
694 outbreaks in India. Outbreaks that occurred during the high incidence period are represented in
695 burgundy and those that occurred during the low incidence period in khaki. The map does not reflect
696 the authors' assertion of territory or borders of any sovereign country including India and is displayed
697 only to present the distribution of JEV occurrence.

698 Figure 3. Japanese encephalitis virus (JEV) outbreak risk based on predicted intensity at 1.0 arc minutes
699 (approximately 2 km). The centre panels depict the distribution of JEV risk for freshwater marsh-
700 fragmented rainfed mosaics (top) and for river-fragmented rainfed mosaics (bottom) models as deciles
701 of the predicted intensities from the best fitting and performing inhomogeneous Poisson point process
702 models (Table 1). The left and right panels depict the lower and upper 95% confidence limits,
703 respectively, for the predicted intensities. The map does not reflect the authors' assertion of territory or
704 borders of any sovereign country including India and is displayed only to present the distribution of JEV
705 occurrence.

706 Figure 4. Homogeneous (left panels) and inhomogeneous (right panels) K-functions for the Japanese
707 encephalitis virus (JEV) outbreak point process. The homogeneous K-function is not an appropriate fit
708 due to the spatial dependency in JEV outbreaks as depicted by the divergent empirical (black line) and
709 theoretical functions (the latter is the theoretical function under complete spatial randomness,
710 represented by the dashed red line with confidence bands in grey). In contrast, the freshwater marsh-
711 fragmented rainfed mosaics (top) and river-fragmented rainfed mosaics (bottom) model-based
712 inhomogeneous K-functions show that the spatial dependency was accounted for by the model
713 covariates (overlapping empirical and theoretical functions). The x-axes, r, represent increasing radii of
714 subregions of the window of JEV outbreaks, while the y-axes represent the K-functions.

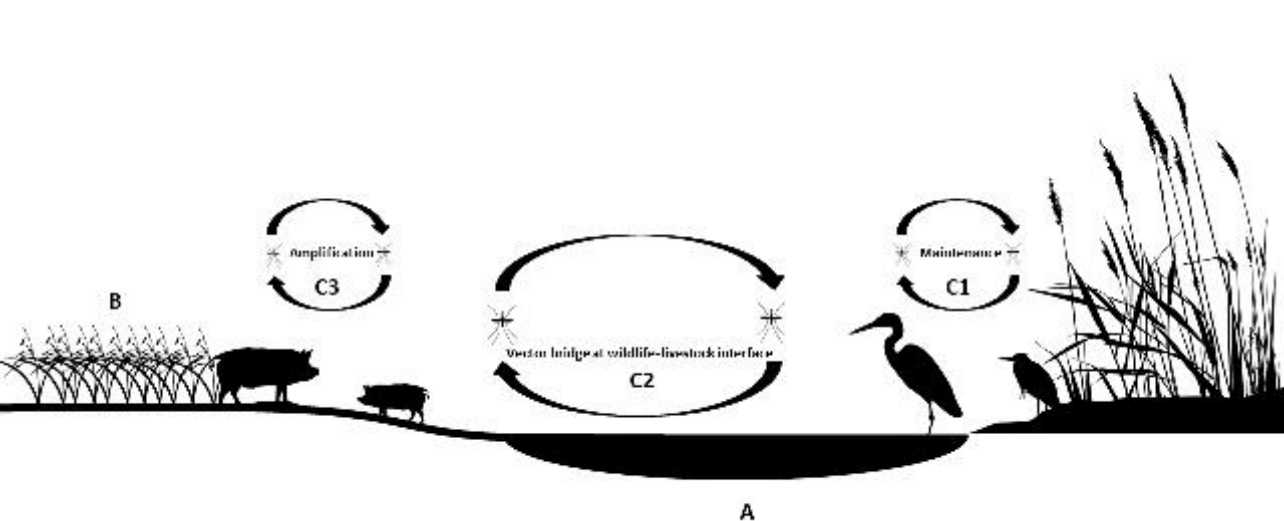
Amplification
C3
Maintenance
C1
Vector bridge at wildlife-livestock interface
C2
B
A

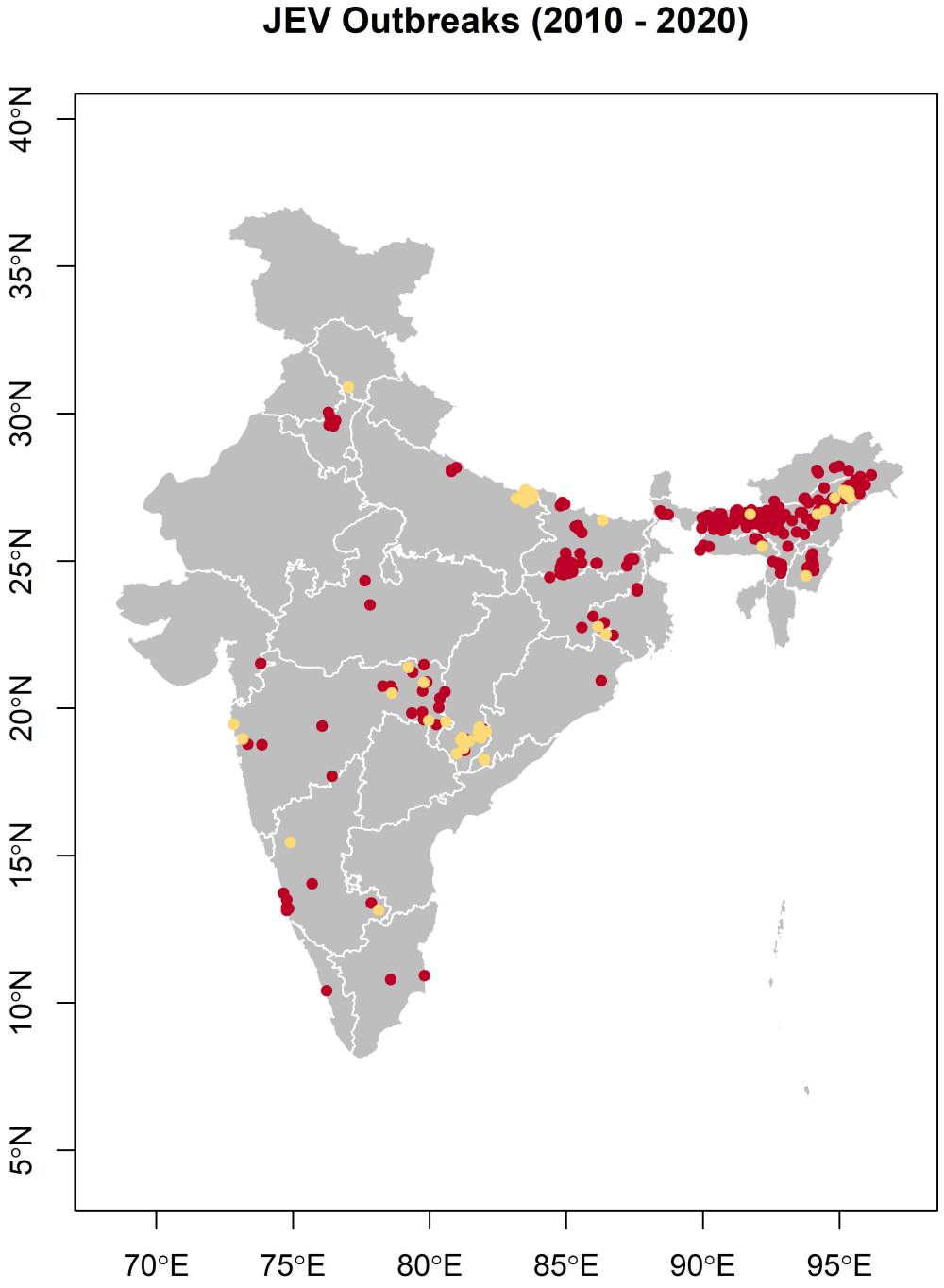
JEV Outbreaks (2010 - 2020)
40°N
35°N
30°N
25°N
20°N
15°N
10°N
5°N
70°E
75°E
80°E
85°E
90°E
95°E

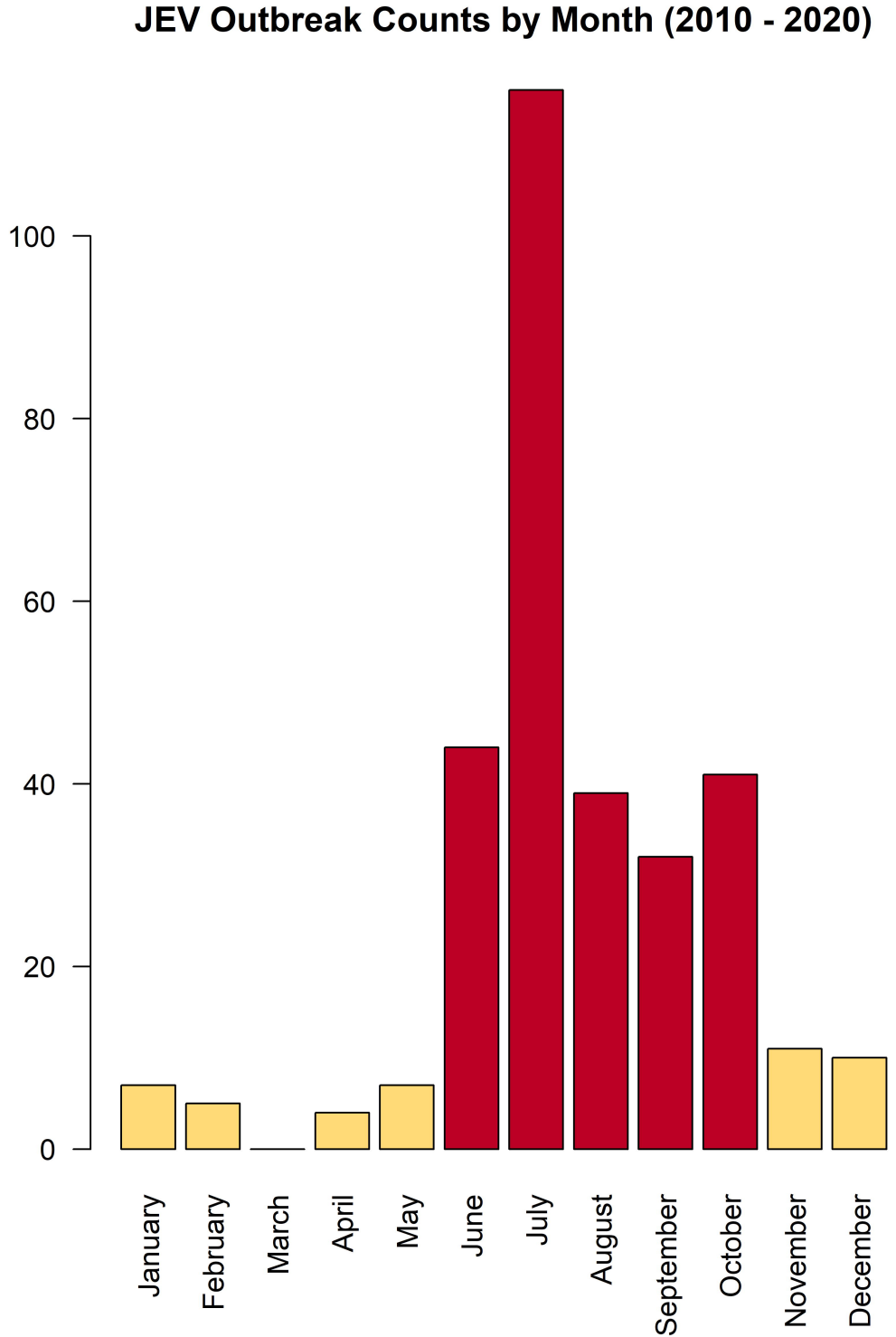
JEV Outbreak Counts by Month (2010 - 2020)
100
80
60
40
20
0
January
February
March
April
May
June
July
August
September
October
November
December

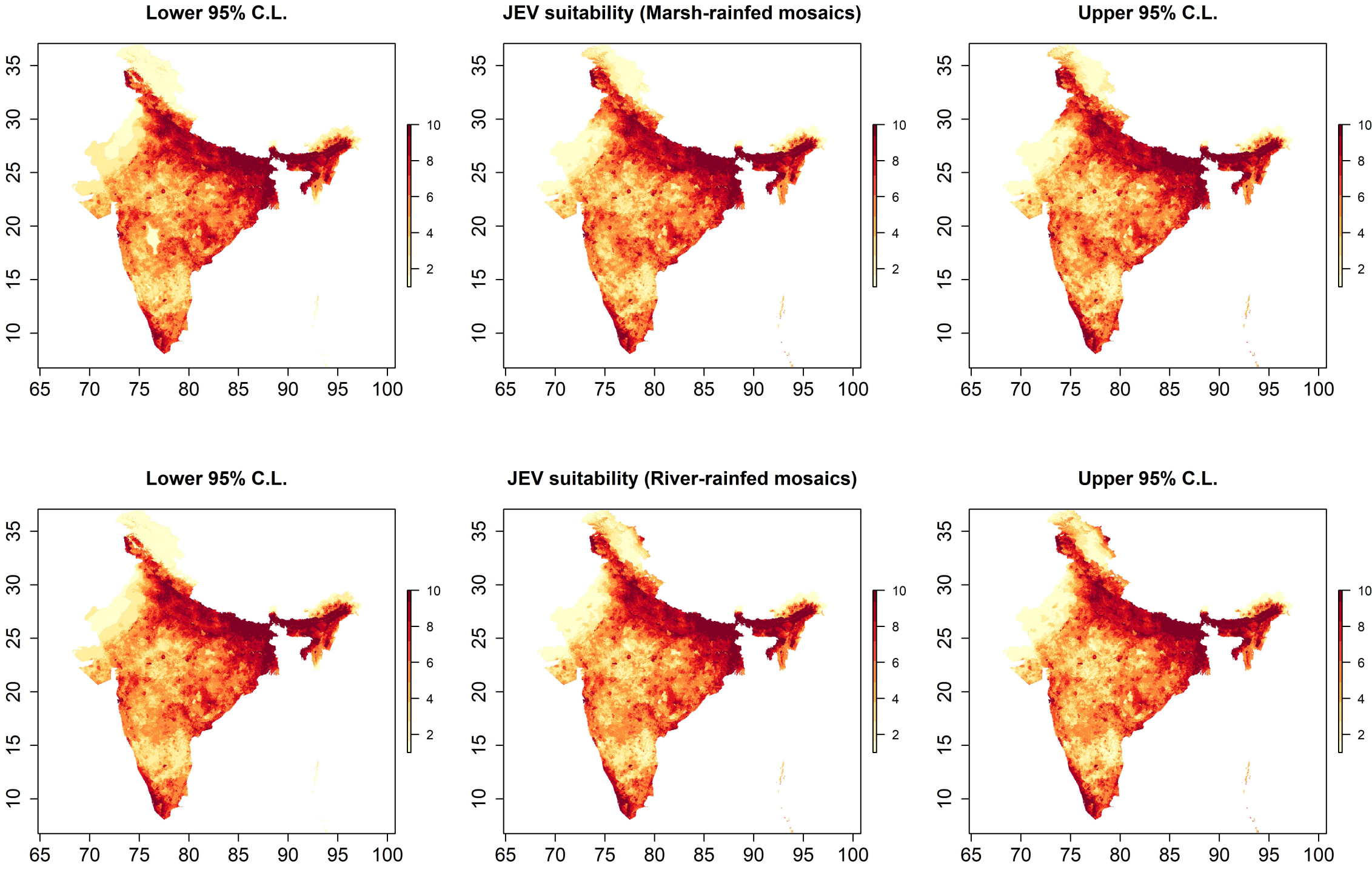
Lower 95% C.L.
JEV suitability (Marsh-rainfed mosaics)
Upper 95% C.L.
Lower 95% C.L.
JEV suitability (River-rainfed mosaics)
Upper 95% C.L.
10
30
25
20
15
65
70
75
80
85
90
95
100
2
4
6
8

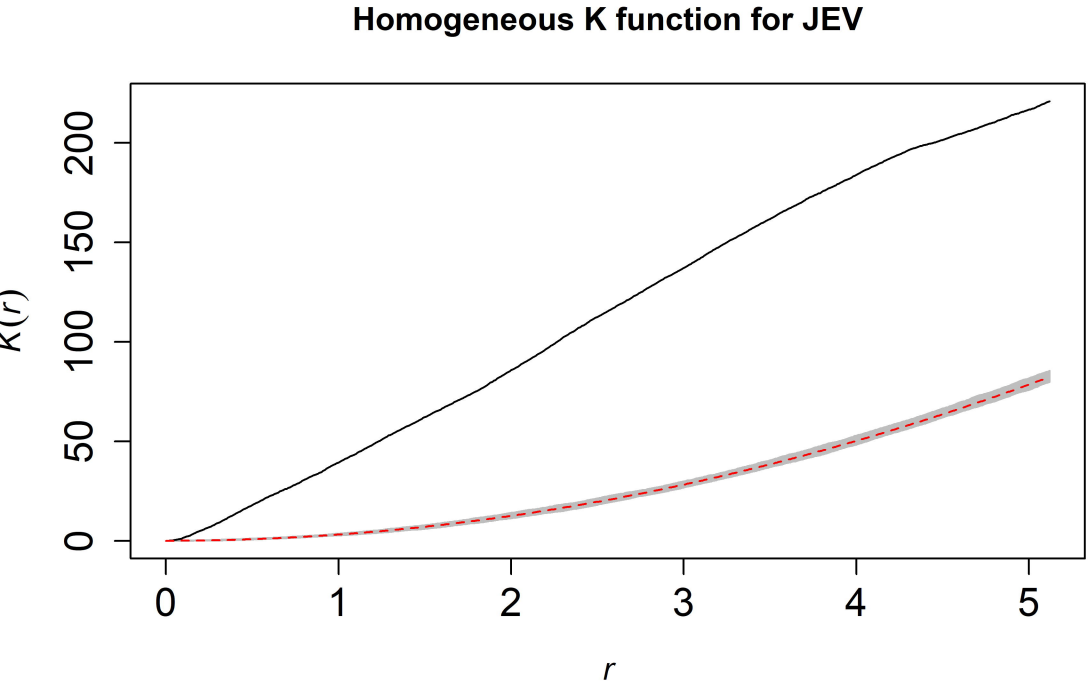
Homogeneous K function for JEV
K(r)
0
50
100
150
200
0
1
2
3
4
5
r

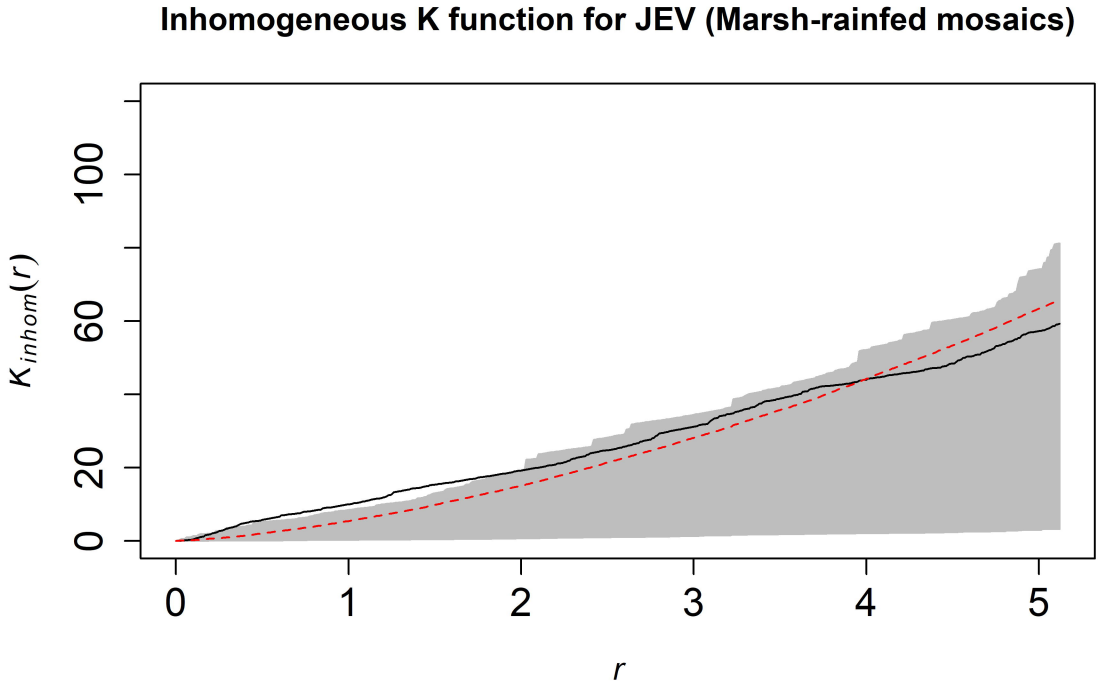
Inhomogeneous K function for JEV (Marsh-rainfed mosaics)
$K_{inhom}(r)$
0
20
60
100
0
1
2
3
4
5
r

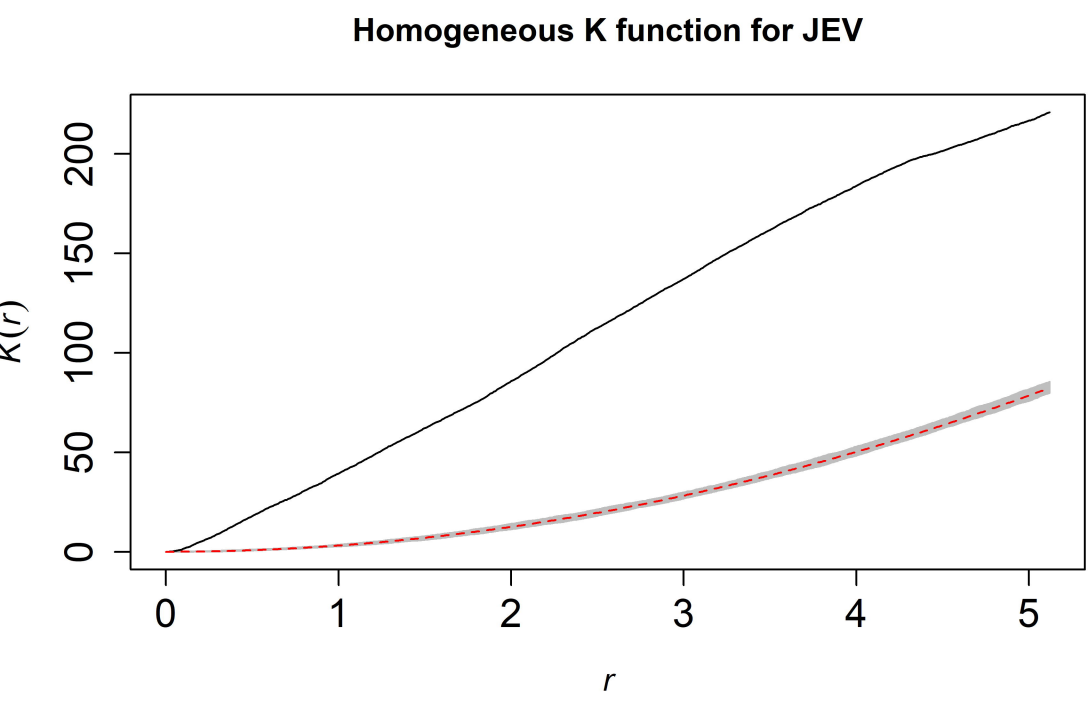
Homogeneous K function for JEV
K(r)
0
50
100
150
200
0
1
2
3
4
5
r

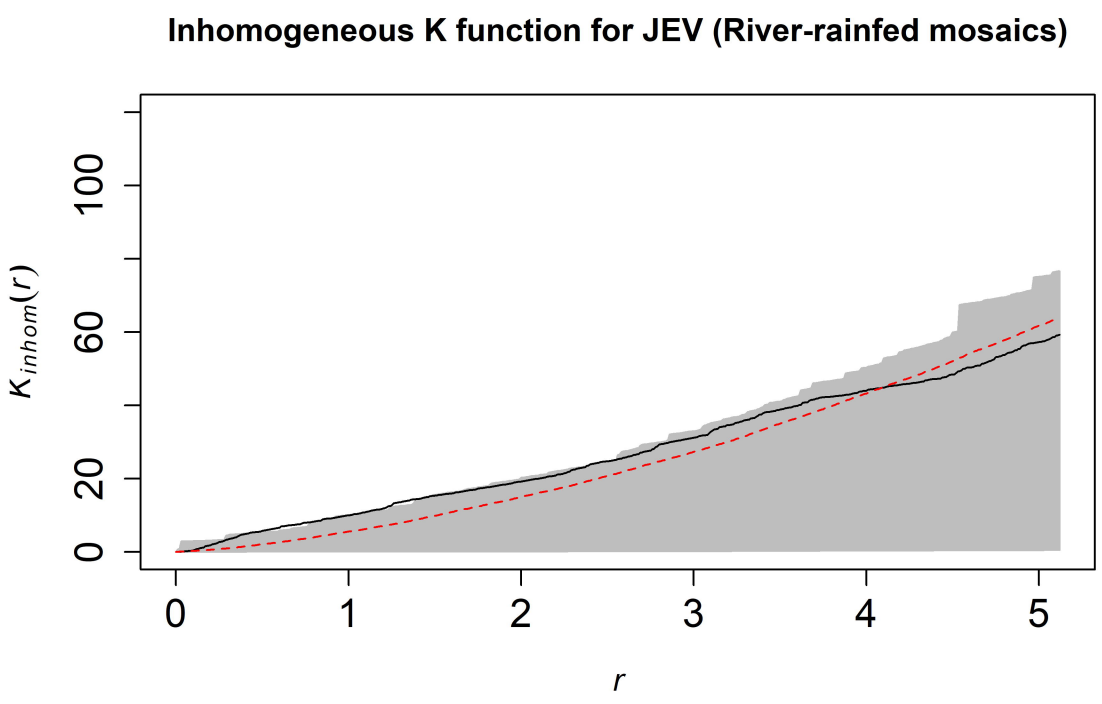
Inhomogeneous K function for JEV (River-rainfed mosaics)
$K_{inhom}(r)$
0
20
60
100
0
1
2
3
4
5
r